Photochemical & Photobiological Sciences (2025) 24:1617–1632
https://doi.org/10.1007/s43630-025-00784-x

RESEARCH

Effect of photobiomodulation therapy on surfactant production increase in human lung epithelial alveolar cells

Halil İbrahim Özdemir[1] · Metin Bilge[5] · Ertuğrul Özkan[5] · Nur Selvi Günel[3] · Hatice Elif Özdemir[2] · Ayshan Ahadova[3] · Ayşe Çekin[3] · Latife Merve Oktay Çelebi[3] · Çağla Kayabaşı[4] · Züleyha Özçelik Çetinel[5] · Duygu Bilge[5] · Murat Koylu[6] · Cansın Şirin Tomruk[7] · Canberk Tomruk[7] · Şenay Şanlıer[8] · Demet Terek[9] · Elif Erol[10] · Fahri Emrah Soylu[11] · Mehmet Yalaz[9] · İsmail Oran[1] · Cumhur Gündüz[3]

Received: 14 July 2025 / Accepted: 21 September 2025 / Published online: 25 September 2025
© The Author(s), under exclusive licence to the European Photochemistry Association, European Society for Photobiology 2025

Abstract
This study aimed to investigate photobiomodulation (PBM) by infrared LED lights as a non-invasive treatment for respiratory distress syndrome in premature and mature newborns, utilizing mature human lung epithelial alveolar cells as a model system. Human lung epithelial alveolar cells were irradiated using liquid-cooled infrared LED setups. Experiments were conducted with three wavelengths (660, 830, 940 nm), two light powers (30, 60 mW), and four energy levels (3, 5, 10, 15 J/cm^2), with exposures at 24, 48, and 72 h. Each experiment was repeated three times. Statistical analysis was performed using one-way ANOVA via GraphPad Prism software, with $p < 0.05$ considered significant. PBM significantly increased surfactant protein levels. Specifically, 660 and 830 nm wavelengths led to over a 50% increase in Surfactant Protein A. Combined 830 and 940 nm irradiation resulted in up to a 150% increase in Surfactant Protein B. PBM at 830 nm increased Surfactant Protein C by nearly 40%. Furthermore, 830 nm and particularly 940 nm irradiations caused approximately a 120% increase in Surfactant Protein D. Photobiomodulation therapy using infrared lights enhanced surfactant protein production in mature human lung epithelial alveolar cells. These findings suggest that this applied method may be a promising non-invasive treatment for respiratory distress syndrome in newborns, addressing a critical gap in current research.

Keywords Respiratory distress syndrome · Alveolar surfactant · Lung epithelial alveolar cells · IR LED/laser therapy · Premature · Photobiomodulation therapy

1 Introduction

Respiratory Distress Syndrome (RDS) predominantly affects preterm and term newborn infants due to a deficiency or structural immaturity of alveolar surfactants in their lungs [1, 2]. Surfactant, a lipid-protein complex, plays a critical role in reducing surface tension, maintaining alveolar stability and regulating airway surface tension. Its composition is approximately 90–95% lipids (predominantly phosphatidylcholine) and 5–10% proteins. The primary component

✉ Nur Selvi Günel
selvi.nur@gmail.com

1 Department of Radiodiagnostics, Faculty of Medicine, Ege University, İzmir, Turkey

2 Department of Norology, Faculty of Medicine, Manisa Celal Bayar University, Manisa, Turkey

3 Department of Medical Biology, Faculty of Medicine, Ege University, İzmir, Turkey

4 Department of Medical Biology, Faculty of Medicine, Balıkesir University, Balıkesir, Turkey

5 Department of Physics, Faculty of Science, Ege University, İzmir, Turkey

6 Department of Radiation Oncology, Faculty of Medicine, Ege University, İzmir, Turkey

7 Department of Histology and Embryology, Faculty of Medicine, Ege University, İzmir, Turkey

8 Department of Biochemistry, Faculty of Science, Ege University, İzmir, Turkey

9 Department of Child Health and Diseases, Faculty of Medicine, Ege University, İzmir, Turkey

10 Clinical Research Associate, IQVIA, Istanbul, Turkey

11 EGEHAYMER, Ege University, İzmir, Turkey

responsible for reducing surface tension is dipalmitoylphosphatidylcholine (DPPC), which constitutes 60% of phosphatidylcholine. The surfactant proteins include SP-A, SP-B, SP-C, and SP-D, with SP-B and SP-C being particularly vital for surface tension reduction. Commercial natural surfactant preparations typically contain SP-B and SP-C. Surfactant deficiency leads to alveolar collapse (atelectasis), which disrupts the ventilation–perfusion balance and impairs gas exchange [3, 4].

Surfactant synthesis begins in type 2 pneumocytes between 20 and 24 weeks of gestation, is stored in lamellar bodies at 24 weeks, and starts being released between 28 and 30 weeks, reaching sufficient levels by 35 to 36 weeks of gestation. Infants born at 28 weeks are at significant risk of developing RDS. Treating surfactant deficiency in RDS is crucial for reducing both mortality and morbidity. Although there is standard treatment for RDS, exogenous surfactant therapy is an invasive procedure associated with severe complications, often requiring prolonged intensive care. While recent developments have introduced non-invasive methods for internal surfactant administration, these also present considerable complications. Additionally, both exogenous and internal surfactant therapies are costly, largely due to the organic nature of surfactant preparations, their short shelf life, and the necessity for cold chain logistics. Common complications include endotracheal tube obstruction, apnea, desaturation, bradycardia, tachycardia, surfactant reflux, volutrauma, pulmonary hemorrhage, unilateral lung surfactant distribution, pneumothorax, and patent ductus arteriosus, all necessitating close monitoring in intensive care units. When the need for repeated surfactant administration is added to the complications, both the costs and risks associated with treatment increase.

Photobiomodulation (PBM) therapy, commonly referred to as "Low-Level Light Therapy" (LLLT), employs infrared (IR-A) light from LEDs or lasers of the 600–1070 nm wavelength, penetrating biological tissues to a certain depth depending on their energy. It has been demonstrated in various studies that it has therapeutic effects on health. The cellular mechanisms activated by PBM include the following [5]:

(1) Effects on mitochondria and cytochrome c oxidase,
(2) Modulation of reactive oxygen species, nitric oxide, and blood flow,
(3) Activation of light-sensitive ion channels and calcium,
(4) Stimulation of transcription factors and signaling pathways, and
(5) Biphasic dose responses and coherence effects in biological systems.

This study explores the potential of non-invasive therapy, low-complication, and external photobiomodulation therapy for the treatment of RDS in preterm infants. Infrared LED light therapy was applied to lung epithelial alveolar cells, and the results were compared with those obtained for the control groups. Due to the lack of preterm lung cell lines, normal human lung alveolar epithelial cell lines were utilized. The study aims to address two key questions:

1) Can infrared photobiomodulation enhance surfactant production in lung cell lines? 2) Which wavelengths of infrared light are most effective in stimulating surfactant production?

2 Materials and methods

2.1 Selection of suitable wavelengths

The selection of infrared light wavelengths was specifically determined considering their interaction with human tissues and the ability to penetrate biological structures. The structures in the human body skin that absorb infrared light include water, hemoglobin, oxyhemoglobin, and melanin pigments. The spectral region known as the "optical window" (wavelengths between 600 and 900 nm), where light absorption is minimal, was identified as optimal for this study (Fig. 1) [6]. To penetrate the skin and reach deeper cells, wavelengths within this range are recommended. Various studies have demonstrated the benefits of photobiomodulation (PBM) for lung inflammatory diseases. For example, De Cunha et al. showed that low-level light therapy (LLLT) at 660 nm (30 mW, 3 J/cm^2) could reduce lung emphysema, airway inflammation, and chronic bronchitis in an experimental COPD animal model [7]. Similarly, Miranda et al. demonstrated that PBM at 660 nm (30 mW, 12 J/cm^2) decreased leukocyte count, mast cell degranulation, myeloperoxidase activity, and microvascular lung permeability in a lung inflammation model induced by formaldehyde exposure [8]. At the final stage of the study, control tests were conducted with doses both below and above the 3 J/cm^2 reference dose. Photobiomodulation applications were repeated on cells at doses of 1, 3, and 5 J/cm^2 and the effects on cell viability, DNA fragmentation, and ATP levels were tested. Statistical analysis was performed using one-way ANOVA with Dunnett's multiple comparisons test; effect sizes were reported as Cohen's d with 95% confidence intervals.

Additionally, Cury et al. found that a single dose of LLLT at 660 nm (30 mW, 10 J/cm^2) could reduce lipopolysaccharide-induced lung inflammation [9]. Beyond these findings, Oliveira et al. demonstrated that PBM at 830 nm (35 mW, 9 J/cm^2) could mitigate acute pulmonary inflammation in both pulmonary and extrapulmonary models of acute respiratory distress syndrome (ARDS) [10]. Based on these findings and the optical window criteria, three wavelengths were selected for the study: 660 nm, 830 nm, and 940 nm.

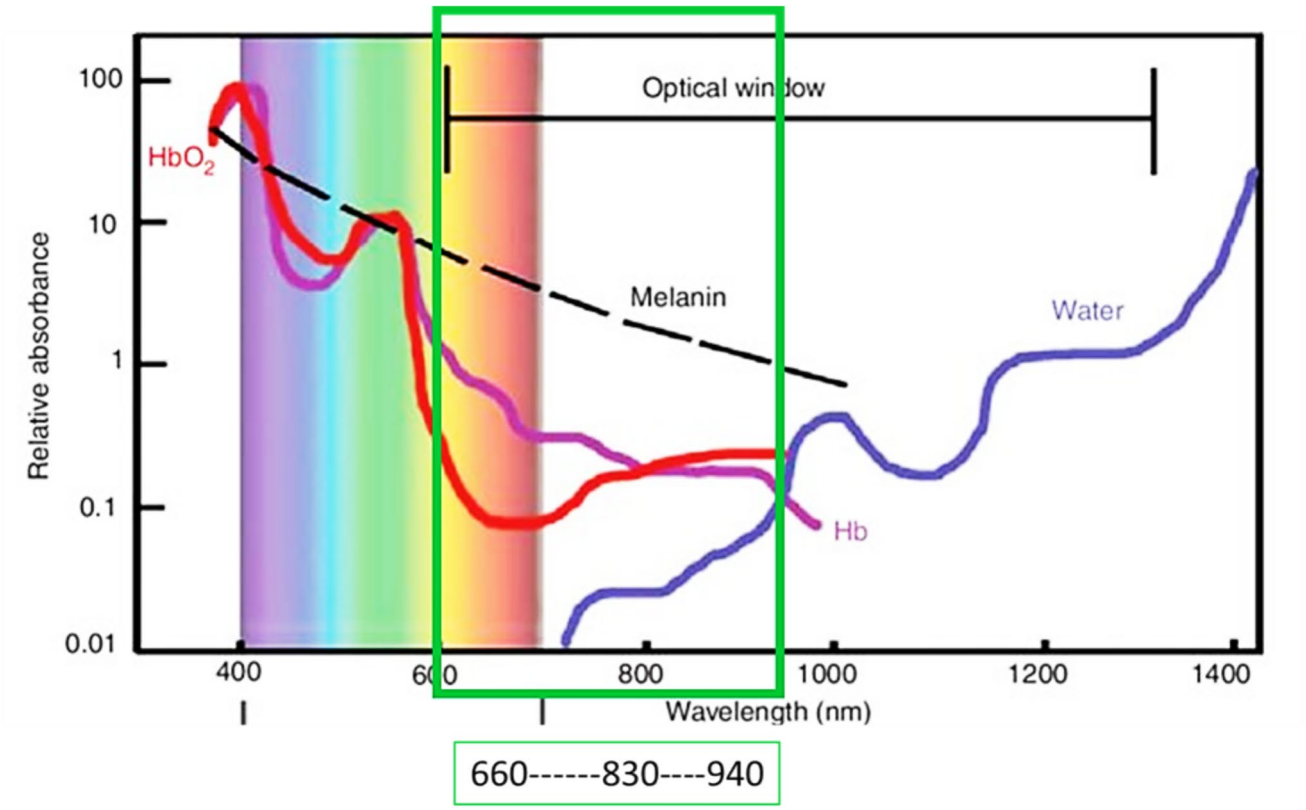

Fig. 1 The optical window showing minimal absorption by hemoglobin, oxyhemoglobin, water, and melanin pigments in the human body (adapted from Lyons et al.) (10)

2.2 Design of LED light setup

The study was conducted within an incubator to maintain cell viability. Initially, the LED setup caused an increase in the incubator's temperature, which was later managed using a liquid cooling system (Fig. 2). The setup was designed using AutoCAD software. M3-threaded holes were drilled into an aluminum cooling block, and 3W 660 nm LEDs were soldered onto star-shaped aluminum circuit boards, which were then affixed to the cooling block using thermal paste.

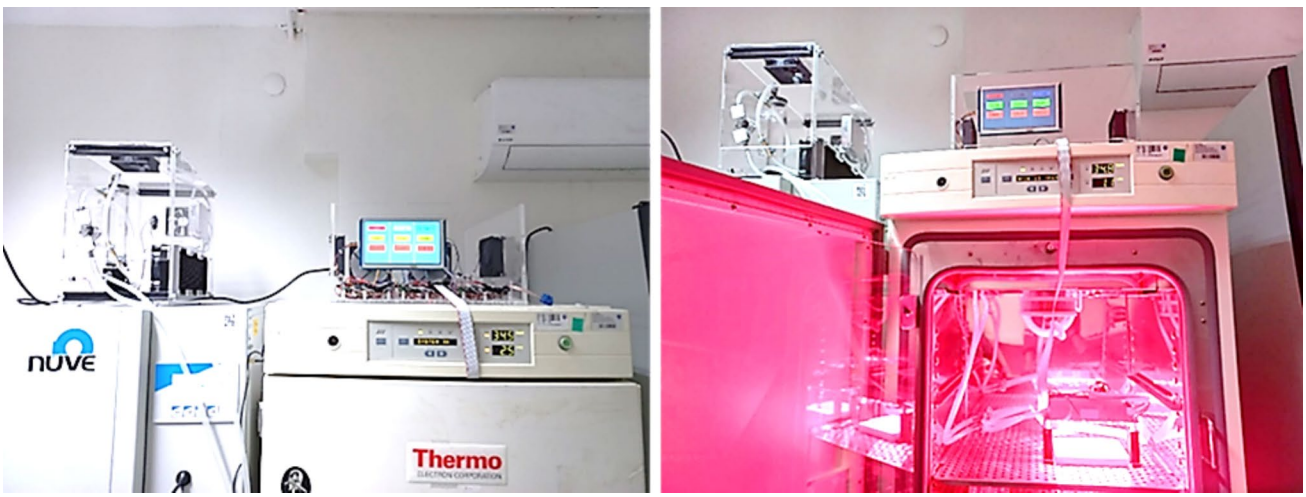

Fig. 2 Placement and application images of the liquid-cooled LED system in the cell culture incubator

A power supply converting 220–12 V, voltage regulators, and LED connections were established to complete the setup (Fig. 3).

Thermal tests were conducted following the assembly. Based on these tests, the LED assemblies were redesigned to be compatible with the liquid cooling system. During this redesign, the positioning of the liquid cooling blocks, mounting brackets, and the new arrangement of the LEDs were carefully considered. The irradiation system was constructed using a 12-V power supply, relay boards, LED driver circuits, a microcontroller board, a real-time clock module, a touchscreen, 92 mm and 120 mm fans, sockets, and switches.

An Arduino Mega was selected as the microcontroller board, programmed using Arduino IDE software. The touchscreen was connected to the microcontroller via the UART communication protocol. User commands were transmitted to the microcontroller, which served as the primary control unit, through this touchscreen. A 7-inch Nextion touchscreen was used for this purpose, programmed using Nextion Editor software. Relay boards were used to provide energy to the liquid-cooled LED assemblies at appropriate times. A real-time clock module that can be adjusted via the DS3231 module connected to the microcontroller was used to ensure the experimental setup operated at desired time intervals according to the times (Fig. 4).

Following the system activation, optical power measurements were taken for the LED groups**,** emitting light at different wavelengths**,** using a Thorlabs S130VC sensor, PM100USB USB interface module, and Thorlabs Optical Power Monitor software. Exposure durations for energy levels of 3, 5, 10, and 15 J/cm^2 were calculated using the formula: Joules = Watts × Seconds (Table 1).

The liquid-cooled LED system was placed inside the cell culture incubator, and red/infrared light applications were performed as indicated in Table 1. Both the electronic system driving the LEDs and the liquid cooling system were supported by uninterruptible power supplies (UPS) to prevent potential adverse effects from power outages and against voltage changes.

2.3 Cell preparation

Due to the unavailability of human preterm lung alveolar cells, mature human epithelial lung alveolar cells were utilized in this study. The human primary alveolar epithelial cell line H-6053 (Cell Biologics, Chicago, USA) was obtained for in vitro studies. Colored well plates were used to prevent light diffusion between the wells. A control group was also included.

The experimental setup was adjusted based on three different light wavelengths (660, 830, and 940 nm), two power levels (30 and 60 mW), and four energy levels (3, 5, 10, and 15 J/cm^2). The cells were exposed to radiation for durations of 24 h, 48 h, and 72 h, and each experiment was repeated 3 times (Table 1). A control group was also included.

Using the microcontroller and timer setup, irradiation programs were formed and executed automatically according to the durations in Table 1. The control wells were covered with aluminum foil to prevent light exposure. To account

Fig. 3 Wired LED setup and its operation

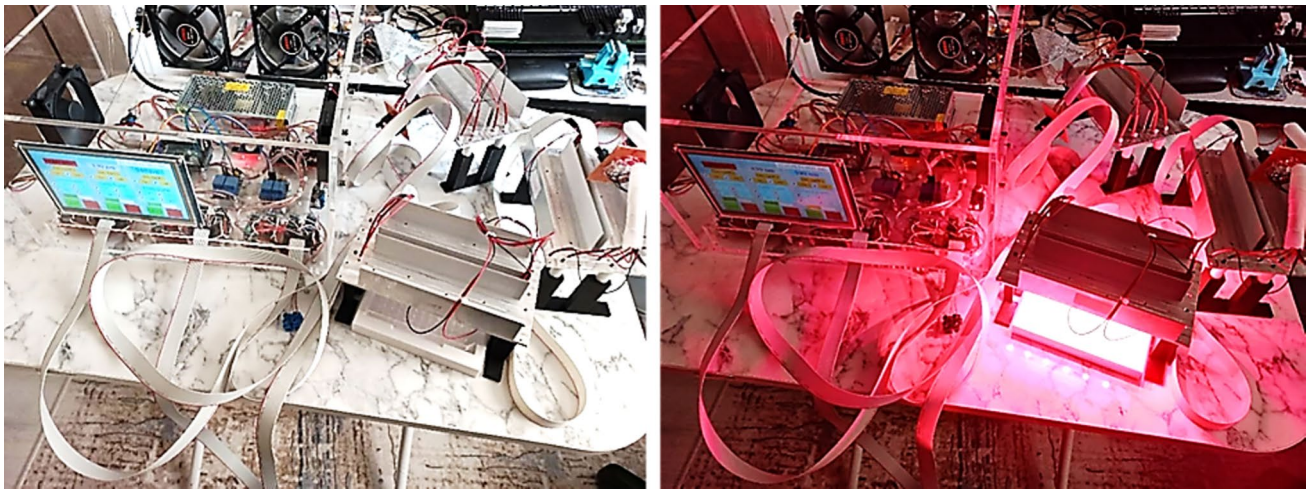

Fig. 4 System components, installation, and operation

Table 1 Unified summary of photobiomodulation (PBM) exposure parameters. (Irradiance (mW/cm^2): The power density measured at the cell culture surface/sample plane. It was measured with a Thorlabs S130VC sensor + PM100USB and Thorlabs Optical Power Monitor software

Condition	Wavelength (nm)	Nominal power (mW)	Irradiance (mW/cm^2)	Energy density (J/cm^2)	Single-session exposure time (s)	Daily repetitions	Total study window
Control	–	–	0	0	0	1/2/3	24/48/72 h
PBM	660	30 I 60	38.7 ± 0.12 I45.5 ± 0.14	3	77	1/2/3	24/48/72 h
				5	129		
				10	258		
				15	387		
PBM	830	30 I 60	40.2 ± 0.11 I45.3 ± 0.12	3	74	1/2/3	24/48/72 h
				5	124		
				10	248		
				15	373		
PBM	940	30 I 60	21.7 ± 0.09 I 43 ± 0.11	3	138	1/2/3	24/48/72 h
				5	230		
				10	460		
				15	691		

for the continuing effects of light exposure, the wells, the irradiation of which was completed, were incubated for an additional 24 h before being tested.

H-6053 cells were cultured in a complete growth medium, which was prepared by adding epithelial cell growth supplement, antibiotic–antimycotic solution, and 10% fetal bovine serum to the "Human Epithelial Cell Medium" (Catalog No: H6621, Cell Biologics). Prior to cell seeding, the flasks and plates were coated with "Gelatin-Based Coating Solution" (Catalog No: 6950, Cell Biologics) for 2 min, and the excess solutions were removed through aspiration.

Cells were incubated at 37 °C in a humidified atmosphere containing 5% CO_2 and monitored using an inverted microscope. When the cells reached approximately 70%, the cells were detached from the flask surface using 0.25% trypsin–EDTA solution, and the trypsin was neutralized with complete growth medium containing serum. The cell suspension was centrifuged at 120 g for 5 min. After centrifugation, the cells were either resuspended in fresh complete growth medium and passaged at a 1:2 ratio or cryopreserved in cold "Cell Culture Freezing Medium" (Catalog No: 6916, Cell Biologics) and stored at −86 °C. Trypan blue dye was used to assess cell viability and to count the cultured cells. Cells with a viability of 95% or higher were used for in vitro experiments.

Changes in surfactant protein (SP-A, SP-B, SP-C, and SP-D) release induced by LED light applications at

different durations, wavelengths, and energy levels were determined using the ELISA method.

Cultured in the dark served as the control group. According to the kit procedure, 40 µl of cell culture supernatants, 10 µl of the relevant antibody, and 5 µl of streptavidin-HRP were added to each ELISA test well. In the ELISA standard wells, 50 µl of the relevant standards (at concentrations of 40, 20, 10, 5, 2.5 ng/ml) and 5 µl of streptavidin-HRP were added. No sample, standard, antibody, or streptavidin-HRP was added to the wells considered as blanks. If any sample, standard, antibody, or streptavidin-HRP is not added to the wells they are considered as blank.

The ELISA plates were covered with a membrane and incubated at 37 °C for 60 min. Washing steps were performed using the washing solution supplied with the kit.

Subsequently, 50 µl of chromogen A, followed by 50 µl of chromogen B solution, were added to each well and incubated in the dark at 37 °C for 10 min. The reaction was terminated by adding 50 µl of stop solution to each well. Optical densities were measured at 450 nm using a microplate reader (Thermo, Multiskan FC) within 15 min. Surfactant protein release levels in the cells subjected to photobiomodulation were compared to those of the control group. All experiments were conducted in triplicate. Differences between groups were analyzed using one-way ANOVA with GraphPad Prism software v.10.0, with a p-value < 0.05 considered significant.

The potential cytotoxicity of LED light application at different durations, wavelengths, and energy levels was assessed in vitro using the real-time cell analysis system (RTCA- xCELLigence, Roche, Berlin, Germany). The photobiomodulation applications commenced 24 h after the cells were seeded into 96-well plates. Impedance recordings were made every 15 min for 72 h after light application using the xCELLigence system.

Cell indices at 24, 48, and 72 h were normalized against control. All experiments were conducted in triplicate. Data were analyzed using the linear quadratic survival model (with the Y-axis expressed as a percentage) in GraphPad Prism software. Additionally, DNA fragmentation was assessed using the TUNEL method with the APO-DIRECT kit. The effect of photobiomodulation on ATP levels was measured using the CellTiter-Glo® Luminescent Cell Viability Assay (Promega) kit.

In the final stage of the study, control tests were conducted by including one lower and one higher dose than the 3 J/cm^2 dose used. Photobiomodulation applications were repeated on cells at doses of 1, 3, and 5 J/cm^2, and the effects on cell viability, DNA fragmentation, and ATP levels were tested. Statistical analysis was performed using one-way ANOVA with Dunnett's multiple comparisons test; effect sizes were reported as Cohen's d with 95% confidence intervals.

3 Results

The cell study demonstrated significant increases in surfactant protein levels across various experimental conditions. Surfactant Protein A (SP-A) levels increased by over 50% in several combinations by applying photobiomodulation therapy (PBMT) at wavelengths of 660 nm and 830 nm. Surfactant Protein B (SP-B) levels increased by up to 150% following PBMT at 830 nm and 940 nm. Notably, the 830 nm combinations led to approximately a 40% increase in Surfactant Protein C (SP-C). Applications at 830 nm and particularly at 940 nm resulted in about a 120% increase in Surfactant Protein D (SP-D) levels. The top three highest increases in surfactant proteins are summarized in Table 2. Considering the wavelength, energy, dose, and their proliferative effects on cells, the 660 nm, 30 mW, 72-h LED application increased surfactant production by an average of 1.25-fold compared to the control (1.00), with a 25% increase in cell proliferation (Fig. 5). Surfactant B and C are components of commercial surfactant preparations used in premature newborns, while Surfactant A and D, which are not present in these preparations, are involved in immune system function and phagocytic activities [11]. Notably, in our photobiomodulation applications, particularly by applying infrared LED treatment at 660 nm and 30 mW, three times daily for three days (72 h), parallel increases were observed in SP-A and SP-D alongside SP-B and SP-C (Table 2, highlighted in bold row).

In our cell viability experiments, photobiomodulation treatments at 660 nm exhibited up to a 25% increase in cell proliferation (Fig. 6). However, the photobiomodulation at 830 nm and higher energy levels was observed to induce up to 25% phototoxicity (Fig. 7). No significant effect on cell viability was detected with the 940 nm wavelength (Fig. 8).

3.1 Photobiomodulation application in cell viability measurements using the xCELLigence method

Cell viability measurements began 24 h after seeding cells into 96-well plates and initiating photobiomodulation treatments. Following the termination of light exposure, the xCELLigence system recorded impedance every 15 min for 72 h. Cell indices at 24, 48, and 72 h were normalized to the control. Analysis was conducted using the GraphPad Prism software with a linear-quadratic survival model (Y-axis expressed as a percentage). Cell viability was assessed at the selected photomodulation dose of 3 J/cm^2, along with one lower and one higher energy level.

Our analysis indicated no cytotoxic effects at 1, 3, and 5 J/cm^2 energy levels in type 2 alveolar cells at the

Table 2 Effect of photobiomodulation under selected exposure conditions on surfactant protein levels. For each combination of wavelength (nm), duration (h), daily repetitions (*t*), power (mW), and energy density (J/cm^2), levels of SP-A, SP-B, SP-C, and SP-D are presented as fold change normalized to the concurrent dark control (control = 1.00)

Wavelength (nm)	Duration (h)	*t* (per day)	Power (mW)	Energy (J/cm^2)	SP-A	SP-B	SP-C	SP-D
660	72	2	30	10	**1.74**	0.79	0.94	0.91
830	72	3	30	5	**1.51**	0.84	1.29	0.90
660	72	3	60	5	**1.33**	1.04	0.93	1.02
830	48	2	30	15	0.79	**2.45**	0.80	1.10
940	48	2	30	15	0.86	**1.87**	0.65	1.14
660	48	1	30	15	1.19	**1.52**	0.61	1.55
830	24	1	60	15	0.73	0.72	**1.39**	1.36
830	72	2	30	3	0.92	0.96	**1.33**	0.78
660	**72**	**3**	**30**	**3**	**1.24**	**1.26**	**1.29**	**1.26**
940	72	1	30	5	1.02	1.02	0.99	**2.22**
940	48	1	30	15	0.96	1.42	0.70	**2.00**
830	24	1	30	15	0.85	0.46	0.85	**1.91**

For each protein, the top three increases are highlighted in bold (ties included)

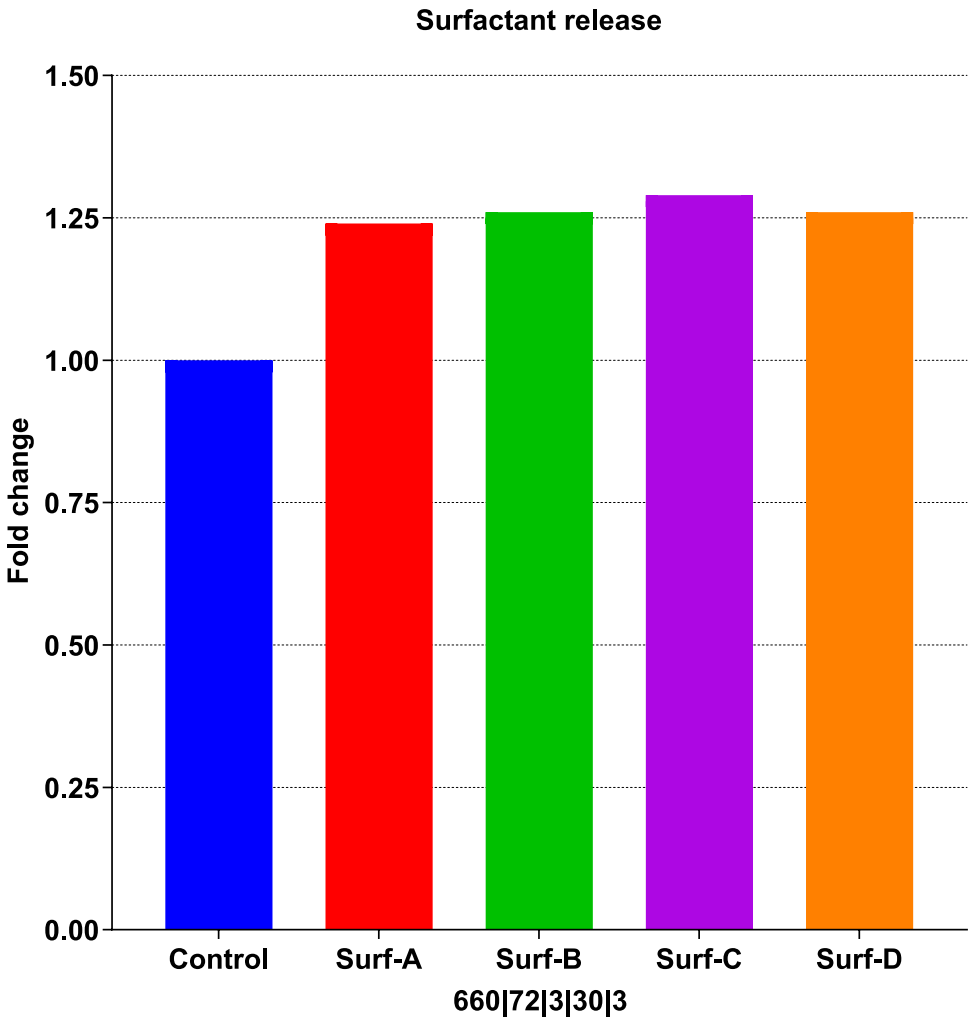

Fig. 5 Effect of infrared photobiomodulation on surfactant protein levels: Levels of SP-A, SP-B, SP-C, and SP-D measured by ELISA in mature human alveolar epithelial cells following LED irradiation at 660 nm, 30 mW, 3 J/cm^2, three times daily for a total of 72 h. Data are normalized to the concurrent dark control and presented as fold change

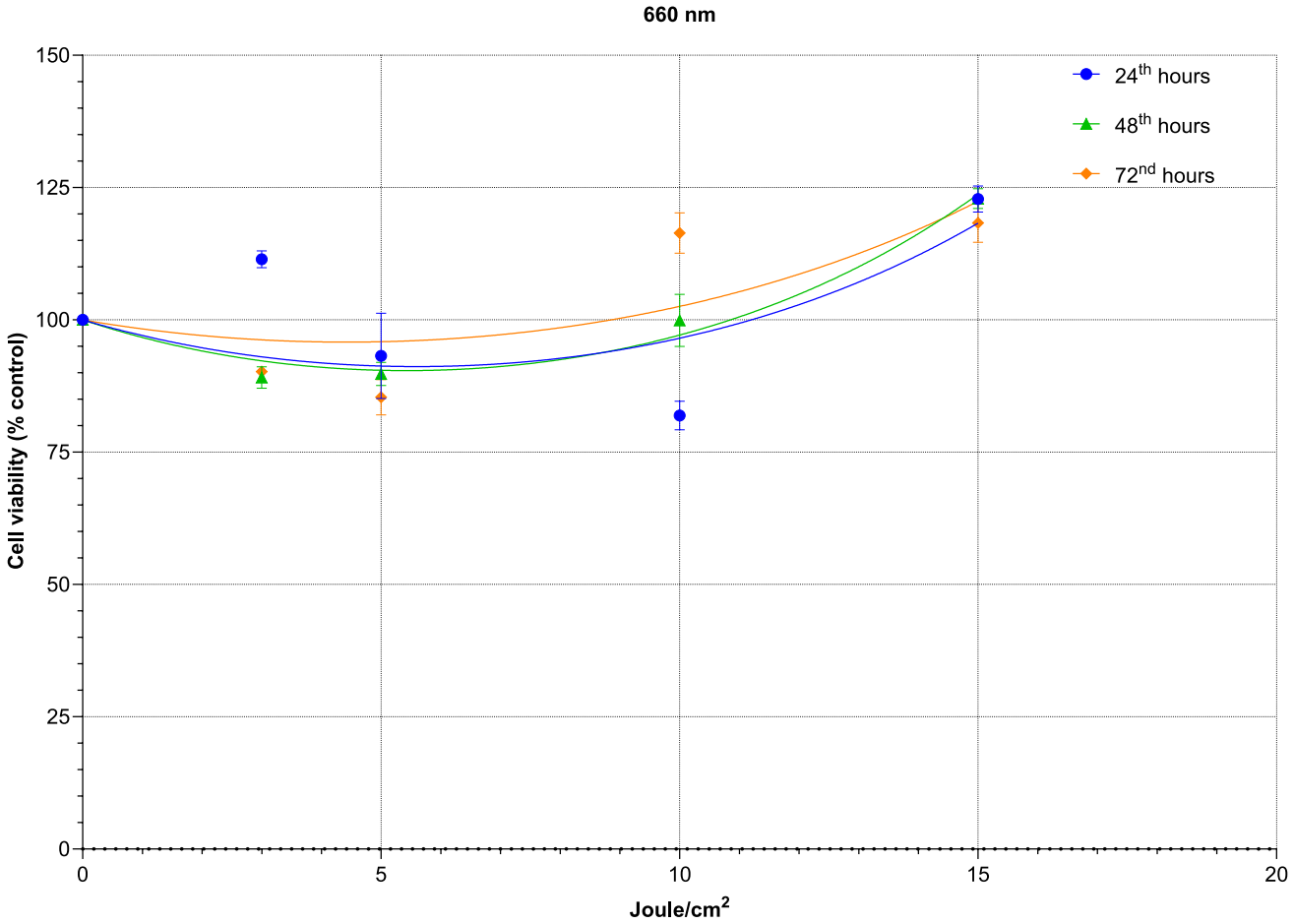

Fig. 6 Effect of photobiomodulation at 660 nm on cell viability. H-6053 human alveolar epithelial cells were irradiated with a 660 nm, 30 mW LED source at energy densities of 1, 3, and 5 J/cm^2; from the start of treatment, the cell index was monitored for 24, 48, and 72 h using the xCELLigence real-time impedance system. Data are normalized to the concurrent dark control and presented as % of control

660 nm and 30 mW dose. Significant increases in cell viability were observed at 24 h compared to the control at 1 ($p = 0.0448$), 3 ($p = 0.0037$), and 5 J/cm^2 ($p = 0.0179$) doses (Fig. 9). At 48 h, significant increases were noted at 3 ($p = 0.0475$) and 5 J/cm^2 ($p = 0.0162$) doses compared to the control, while the 1 J/cm^2 application did not show a significant increase (Fig. 10). At 72 h, significant increases were observed at 1 ($p = 0.0448$), 3 ($p = 0.0037$), and 5 J/cm^2 ($p = 0.0179$) doses compared to the control (Fig. 11). The 3 J/cm^2 energy level demonstrated significant increases at all three time points (24, 48, and 72 h).

3.2 Measurement of the effect of photobiomodulation on DNA fragmentation using the TUNEL method

Apoptotic DNA fragmentation following photobiomodulation in type 2 alveolar cells was measured using the APO-DIRECT kit (BD Pharmingen). Cells were collected 24 h after photobiomodulation and washed with PBS. Cells not subjected to photobiomodulation were used as the control group. After washing, cells were fixed with 1% paraformaldehyde and incubated in ice-cold 70% methanol. After further washing steps, cells were incubated in staining solution containing reaction buffer, TdT enzyme, and FITC-dUTP. Following additional washing, PI/RNase staining buffer was added, and cells were analyzed by flow cytometry within 3 h. Apoptotic changes potentially induced by photobiomodulation were compared with the control group. No apoptotic DNA fragmentation was observed in type 2 alveolar cells, indicating that our photobiomodulation application did not induce apoptosis in alveolar cells (Fig. 12).

3.3 Measurement of the effect of photobiomodulation on ATP levels

Given the correlation between surfactant expression levels in human lung type 2 alveolar epithelial cells and ATP

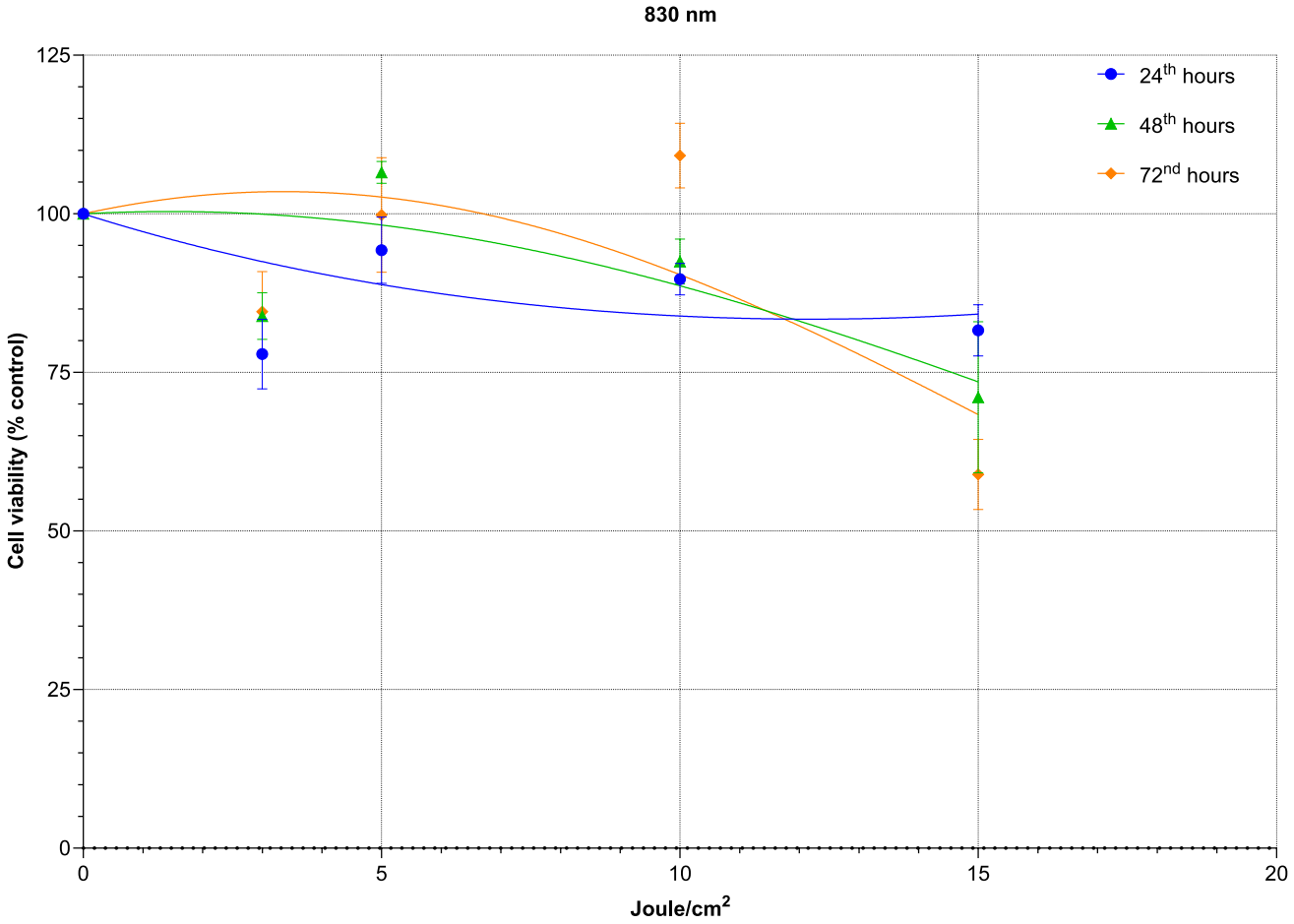

Fig. 7 Effect of photobiomodulation at 830 nm on cell viability. H-6053 human alveolar epithelial cells were irradiated with an 830 nm LED source at selected energy densities; from the start of treatment, the cell index was monitored for 24, 48, and 72 h using the xCELLigence real-time impedance system. Data are normalized to the concurrent dark control and presented as % of control

levels, ATP levels were measured as a complementary parameter. Lung type 2 alveolar epithelial cells were seeded at 10^4 cells/well into 96-well plates, and photobiomodulation doses were applied 72 h later. No treatment was applied to control group cells. ATP levels were measured 72 h post-photobiomodulation using the CellTiter-Glo® Luminescent Cell Viability Assay (Promega) kit according to the manufacturer's instructions with a Thermo Varioskan multi-plate reader (485–500 nm). Our results showed that photobiomodulation at 3 J/cm^2 did not result in an increase in ATP levels, even when tested with one lower and one higher dose (Fig. 13). However, considering that a potential increase in ATP may have been utilized for surfactant production and other cellular activities, the absence of an ATP increase was deemed consistent with expectations. The lack of a decrease in ATP levels, coupled with the observed increase in cell viability, supports this interpretation.

4 Discussion

Surfactants, surface-active compounds, are essential for the proper functioning of the lungs; their production and secretion are regulated by respiratory epithelial cells. In cases of premature birth, type I and type II alveolar cells may not fully develop, and in instances of respiratory tract damage or infection, these cells can be impaired, leading to insufficient surfactant production. Exogenous surfactant therapy is typically the only treatment available for infants in the first hours following premature birth. However, this treatment is invasive and complex. Our hypothesis posits that the application of infrared photobiomodulation externally could reactivate underdeveloped or damaged cells, stimulating them to produce surfactants. The results of our study support this hypothesis, particularly demonstrating that the 660 nm red/infrared light wavelength can enhance

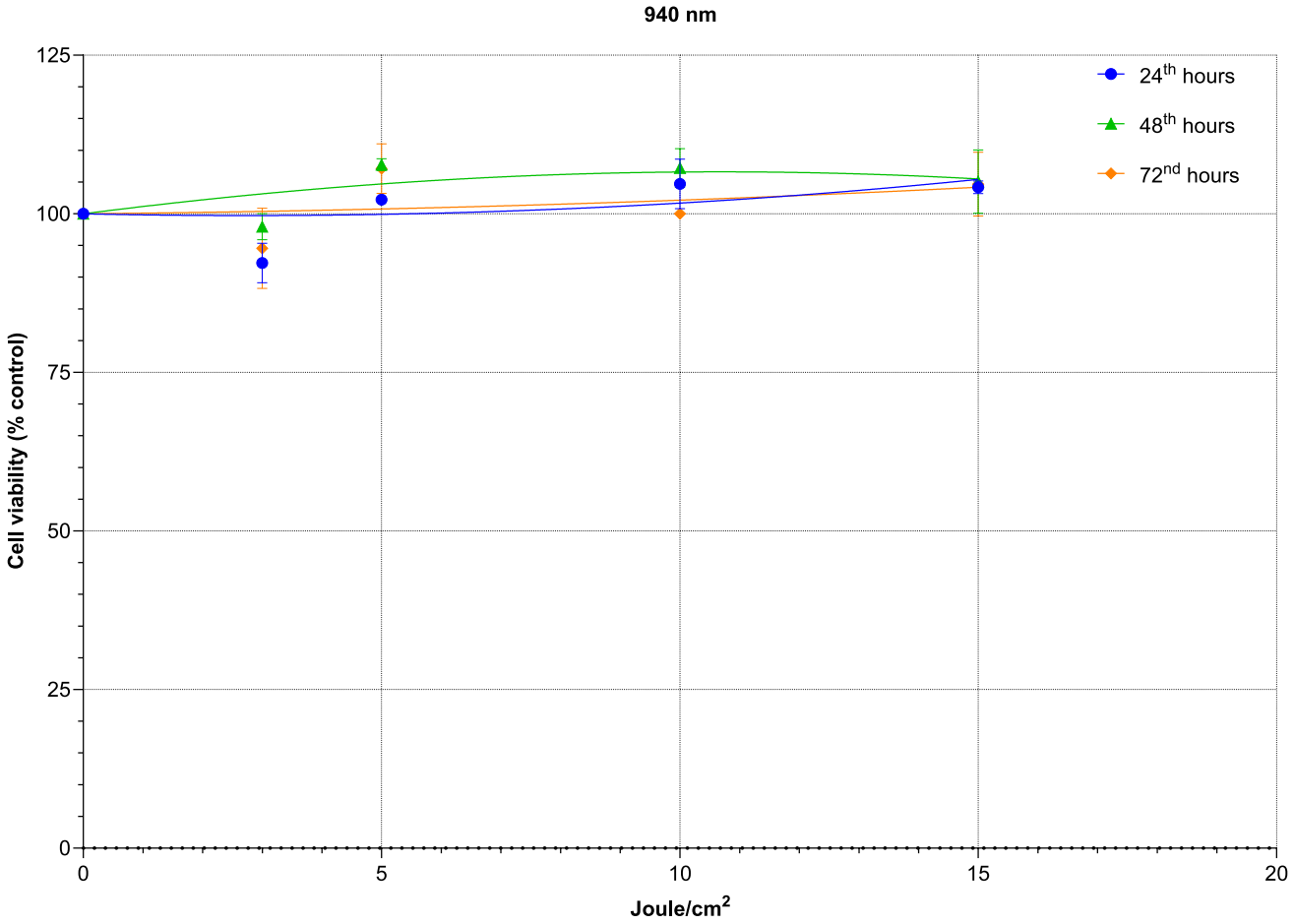

Fig. 8 Effect of photobiomodulation (PBM) at 940 nm on cell viability. H-6053 human alveolar epithelial cells were irradiated with a 940 nm LED source at selected energy densities; from the start of treatment, the cell index was monitored for 24, 48, and 72 h using the xCELLigence real-time impedance system. Data are normalized to the concurrent dark control and presented as % of control

surfactant production even in mature cells. This increase in surfactant production can be attributed to the effect of red/infrared light on mitochondrial function within cells. Mitochondria are the energy-producing organelles of cells, and light at these wavelengths can stimulate mitochondrial activity by enhancing the function of the cytochrome c oxidase enzyme. This stimulation increases ATP production, thereby accelerating cellular metabolism. As surfactant production and release are closely tied to the metabolic activity of respiratory epithelial cells, photobiomodulation with red/infrared light may support surfactant production by boosting the metabolic activity of these cells. Additionally, light at these wavelengths may influence DNA, RNA, and protein synthesis, potentially increasing the activity of genes involved in surfactant production [5].

Currently, no studies in the literature have specifically investigated the effects of infrared photobiomodulation at different doses on cellular surfactant levels. However, Cury et al. examined the anti-inflammatory effects of various doses (1, 3, 5, and 7.5 J/cm^2) of 660 nm light in an in vivo study. They found that the most significant suppression of inflammatory mediators IL-1β and TNF-α in the lungs was achieved at a dose of 7.5 J/cm^2, while IL-6 levels were similarly suppressed across all doses [9]. Cunha et al. also demonstrated the efficacy of photobiomodulation at 660 nm, 30 mW, and 3 J/cm^2, which are the same parameters found effective in our study, in an experimental COPD animal model [7]. In our study, we observed an average increase of 25% in all surfactant proteins by the application of photobiomodulation at a wavelength of 660 nm, a power output of 30 mW, and a dose of 3 J/cm^2, administered three times daily for three days.

Aquide et al. emphasized that the 720–750 nm infrared therapy they used in COVID-19 patients is economical, easy to apply, has no known side effects, and is well-suited for cell culture models [12]. Similarly, our application method is both simple and cost-effective, and we observed no phototoxic effects in cells treated with the 660 nm wavelength. In another study by Aquide et al., using near-infrared (NIR) 730 nm infrared light on human type II alveolar epithelial

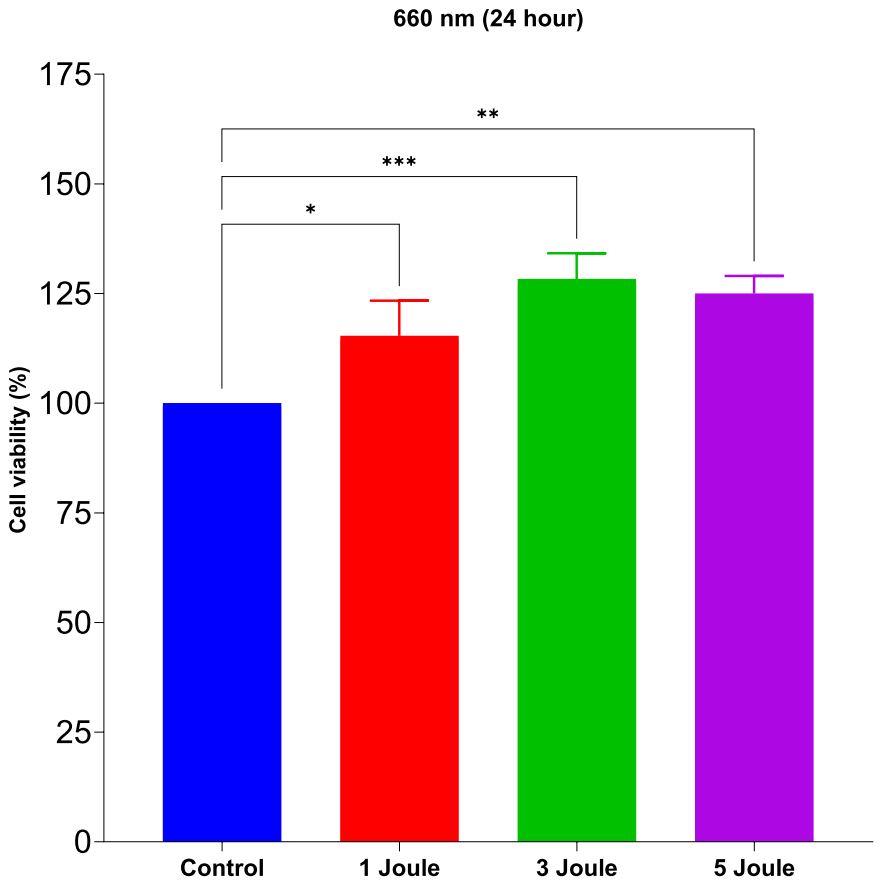

Fig. 9 Cell viability at 24 h in the 660 nm photomodulation control test. H-6053 human alveolar epithelial cells were irradiated at 660 nm with energy densities of 1, 3, and 5 J/cm^2; viability at 24 h post-irradiation was measured using the xCELLigence system, normalized to the concurrent dark control, and presented as % of control. Bars/symbols represent the mean of three independent experiments ($n = 3$), and error bars denote the standard deviation; the dashed horizontal line indicates 100% (control). Statistical analysis was performed using one-way ANOVA (Dunnett's multiple comparisons test); effect sizes were reported as Cohen's *d* with 95% CIs

Dunnett's multiple comparisons test	Summary	Adjusted p	Cohen's *d* (95% CI)
Control vs. 1 Joule	*	0.0200	1.91 (-0.17 to 3.94)
Control vs. 3 Joule	***	0.0005	4.83 (0.55 to 9.39)
Control vs. 5 Joule	**	0.0012	6.25 (0.82 to 12.09)

cells, several key findings were reported: 1) NIR light reduces inflammation in human alveolar and macrophage cells, 2) it reduces inflammation triggered by the SARS-COV-2 spike protein, 3) it stimulates mitochondrial metabolic activity, 4) single exposure to NIR light increases ROS in inflamed cell cultures, 5) consecutive NIR light exposures decrease intracellular ROS, and 6) NIR light regulates genes associated with ROS-clearing enzymes [13]. Additionally, the two case reports suggest the use of photobiomodulation therapy in adult ARDS patients [14], and one research article explores its application in COVID-19. Conversely, it was found in our study that photobiomodulation at 830 nm caused up to 25% phototoxicity at higher doses [15], despite previous reports given by Oliveira et al. suggesting benefits of the 830 nm wavelength in lung applications [10].

The infrared light wavelengths of 660, 830, and 940 nm used in our study significantly increased at least one of the surfactants' proteins by up to 2.5-fold. However, in some instances, a decrease in surfactant production was observed. Regarding cell viability, PBMT at 830 and 940 nm wavelengths decreased cell viability, while PBMT at 660 nm wavelength increased cell viability. Therefore, our application of the 660 nm wavelength at 30 mW power, three times daily for three days, with an energy density of 3 J/cm^2, resulted in an average 25% increase in all surfactant proteins. As a follow-up, our research on premature rat pups is ongoing. Should the results be positive, they will be published in a future study report.

In this study, we observed that 660 nm photobiomodulation produced consistent increases in the surfactant proteins SP-A, SP-B, SP-C, and SP-D, whereas 830 nm and 940 nm yielded more variable responses and, at higher doses, signs of phototoxicity. These findings can be explained by wavelength-dependent interactions among tissue optics, target chromophores, and delivered dose. Within the red/near-infrared "optical window" (~600–1100 nm), scattering tends to decrease with wavelength, but absorption is dictated by the spectra of specific biotissue chromophores: hemoglobin/

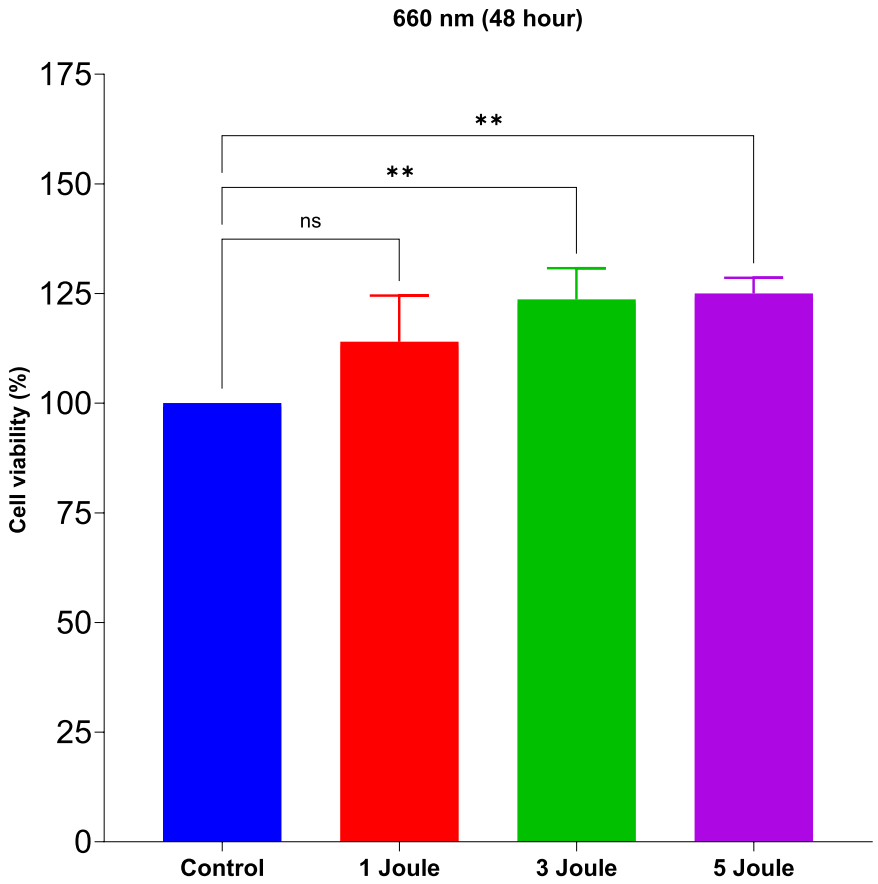

Fig. 10 Cell viability at 48 h in the 660 nm photomodulation control test. H-6053 human alveolar epithelial cells were irradiated with a 660 nm, 30 mW LED source at energy densities of 1, 3, and 5 J/cm.^{2}; post-irradiation viability was measured using the xCELLigence real-time impedance system and presented as % of control after normalization to the concurrent dark control. Bars/symbols represent the mean of three independent experiments ($n = 3$), and error bars denote the standard deviation; the dashed horizontal line indicates 100% (control). Statistical analysis was performed using one-way ANOVA with Dunnett's multiple comparisons test; results are reported with exact adjusted *p*-values and effect sizes (Cohen's *d*, 95% CI)

Dunnett's multiple comparisons test	Summary	Adjusted p	Cohen's *d* (95% CI)
Control vs. 1 Joule	ns	0.0760	1.33 (-0.37 to 2.93)
Control vs. 3 Joule	**	0.0059	3.34 (0.21 to 6.58)
Control vs. 5 Joule	**	0.0043	6.93 (0.95 to 13.40)

melanin absorption declines across 600–700 nm, while water absorption rises beyond ~ 900 nm. Consequently, at 660 nm both superficial losses and competing absorbers are comparatively lower than at longer wavelengths, yielding a more predictable fluence at the cellular plane and, in turn, more reproducible biological effects [16]. Consistent with our data, prior pulmonary models have shown that 660 nm PBM can suppress inflammatory cytokines, mitigate cellular infiltration, and preserve function [7, 9]. At the mechanistic level, cytochrome-c oxidase (CCO)—a principal photoreceptor in PBM—exhibits action-spectrum maxima near ~ 660 nm and ~ 810–830 nm, suggesting that both bands can be bioenergetically effective. However, the light penetrates deeper at a wavelength of 830 nm; thus, for the same nominal energy density (J/cm^2), the actual irradiance (mW/cm^2) incident on the target layer and the local thermal load may be higher, especially in thin culture systems. Therefore, outcomes can be shifted from the stimulatory limb of the biphasic (hormetic) dose–response toward the inhibitory limb, manifesting as reduced viability or frank phototoxicity when the irradiance–time product is not carefully titrated [17, 18]. Our observations at 830 nm are therefore consistent with the broader hormesis literature and underscore the need to report—and to control—irradiance at the sample plane, not merely total energy. By contrast, at ~ 940 nm the absorption spectrum of water becomes increasingly dominant (with a peak near 970–980 nm), whereas this band lies off-peak for CCO. As a result, energy deposition at 940 nm is more readily captured by bulk water, potentially increasing non-specific thermal effects while diminishing targeted photobiomodulation signaling. This optical competition provides a plausible explanation for the attenuated surfactant responses and the neutral or negative viability effects we observed at some 940 nm settings [19, 20]. While this study provides strong proof-of-concept evidence, it also has several methodological and biological limitations. First, we used non-immortalized primary H-6053 alveolar epithelial cells, which may constrain long-term and large-scale reproducibility due to donor/lot variability and limited proliferative capacity. Future work should incorporate immortalized

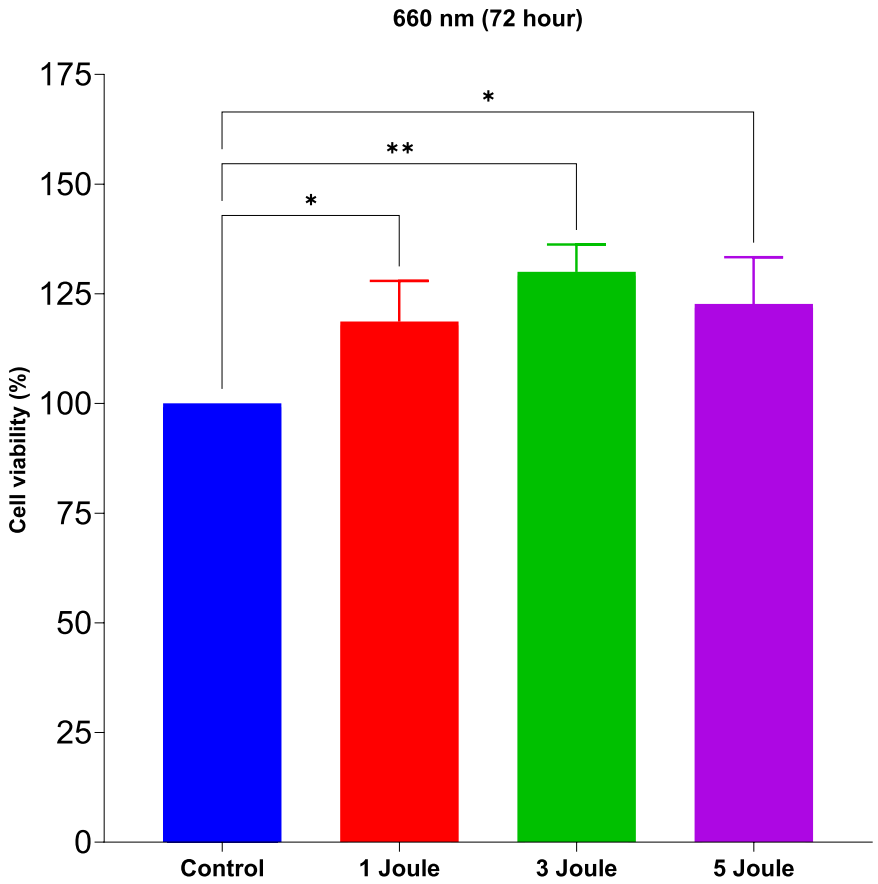

Fig. 11 Cell viability at 72 h in the 660 nm photomodulation control test. H-6053 human alveolar epithelial cells were irradiated with a 660 nm, 30 mW LED source at energy densities of 1, 3, and 5 J/cm^2; post-irradiation viability was monitored using the xCELLigence real-time impedance system and presented as % of control after normalization to the concurrent dark control. Bars/symbols represent the mean of three independent experiments ($n = 3$), and error bars indicate the standard deviation; the dashed horizontal line denotes 100% (control). Statistical analysis was performed using one-way ANOVA with Dunnett's multiple comparisons test; effect sizes for pairwise comparisons are reported as Cohen's *d* with 95% CI

Dunnett's multiple comparisons test	Summary	Adjusted P	Cohen's *d* (95% CI)
Control vs. 1 Joule	*	0.0448	2.01 (-0.14 to 4.12)
Control vs. 3 Joule	**	0.0037	4.80 (0.54 to 9.34)
Control vs. 5 Joule	*	0.0179	2.12 (-0.10 to 4.33)

AT2-like lines or iPSC-derived SFTPC$^+$ alveolar cells, ideally in air–liquid interface and/or 3D organoid systems to enhance physiological relevance and reproducibility. Second, mechanistic conclusions were supported primarily by phenotype-level readouts and literature; direct assessments of mitochondrial bioenergetics were not performed. To substantiate the proposed PBM mechanisms, studies should include mitochondrial ROS (MitoSOX), membrane potential (JC-1/TMRM), oxygen-consumption/extracellular acidification (OCR/ECAR; Seahorse), and cytochrome-c oxidase activity. Third, although surfactant proteins were quantified by ELISA, functional surfactant activity (surface-tension measurements via pulsating-bubble surfactometry/Wilhelmy balance) and molecular confirmations (RT-qPCR/Western blot) were not conducted. Fourth, wavelength–irradiance uniformity may be influenced by well geometry and cooling architecture; detailed beam/dosimetry mapping and microthermal monitoring would mitigate these sources of bias. Finally, the work is limited to in vitro, single-cell-type circumstances; validation in co-cultures (alveolar macrophages/fibroblasts), preterm-like cell models, and in vivo systems (premature rodent models) is required. Although we partially address statistical robustness by reporting effect sizes and 95% confidence intervals alongside *p*-values, multi-center, staged validation will be necessary to establish clinical generalizability.

As a result, this study is one of the first in the literature to specifically investigate the effects of infrared PBM at different doses on cellular surfactant levels. Considering the invasive and complicated nature of existing surfactant therapy, our study aimed to explore the potential of a non-invasive, low-complication, external PBM treatment. The results obtained demonstrated that, in particular, the 660 nm wavelength led to a balanced increase in all surfactant proteins. These findings are thought to fill a gap in the literature in this area. Furthermore, for the first time in this study, the safety and mechanism of PBM were thoroughly investigated through control tests on cell viability, DNA fragmentation, and ATP levels. The detailed results obtained from this study are thought to reveal the potential

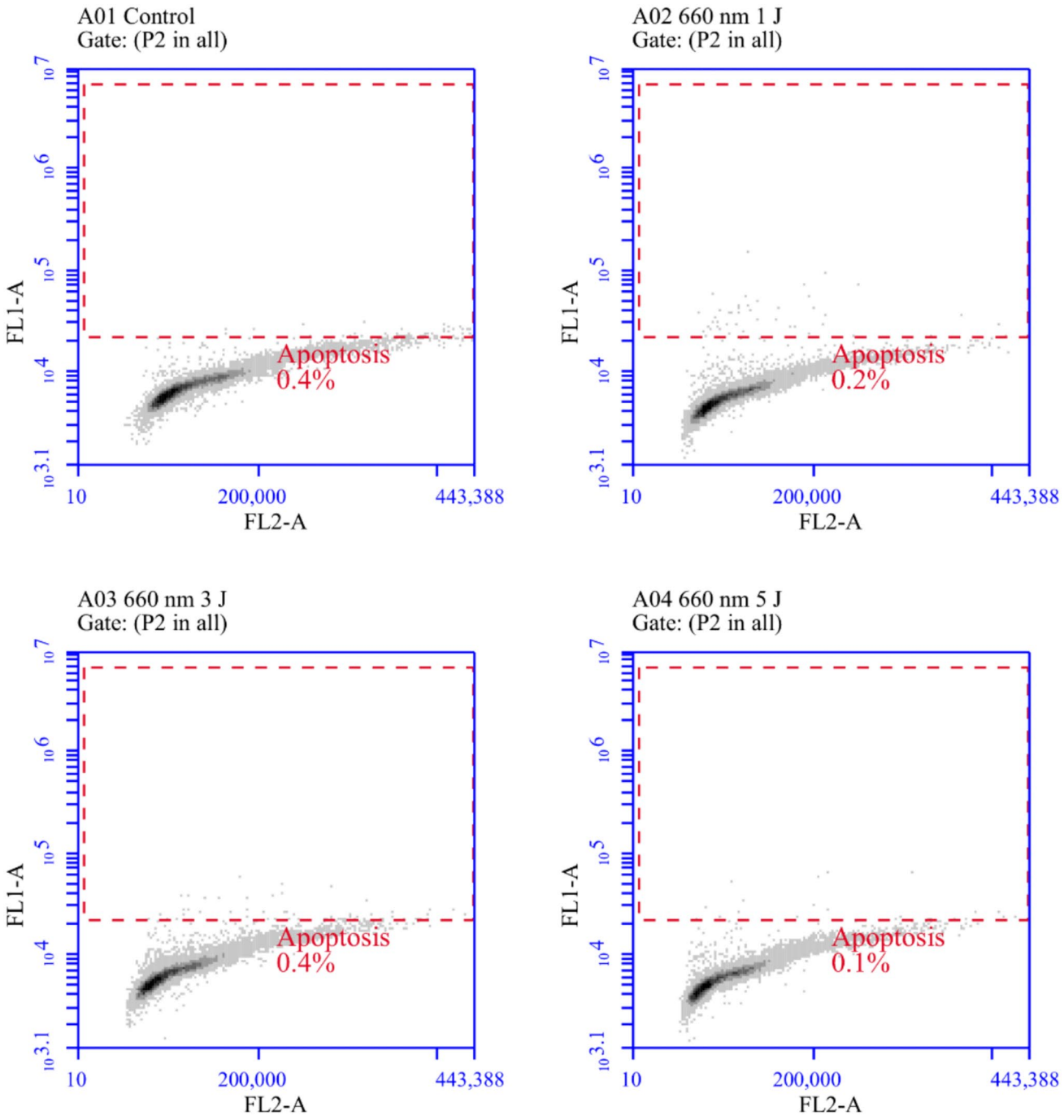

Fig. 12 Control tests for DNA fragmentation by the TUNEL method (660 nm; 1, 3, and 5 J/cm^2). In H-6053 human alveolar epithelial cells, apoptotic DNA fragmentation 24 h after photobiomodulation was assessed using the APO-DIRECT TUNEL kit (FITC-dUTP/TdT) with PI/RNase staining, and cells were analyzed by flow cytometry

of the PBM method, when applied in the treatment of respiratory distress syndrome in newborns, to increase treatment success. This pioneering work paves the way for a paradigm shift in neonatal respiratory care, offering a gentle yet powerful alternative to current invasive interventions.

5 Conclusion

Infrared light applied using the photobiomodulation technique has been shown to increase surfactant protein production in mature human lung epithelial alveolar cells. In particular, the 660 nm wavelength light, which lies at the

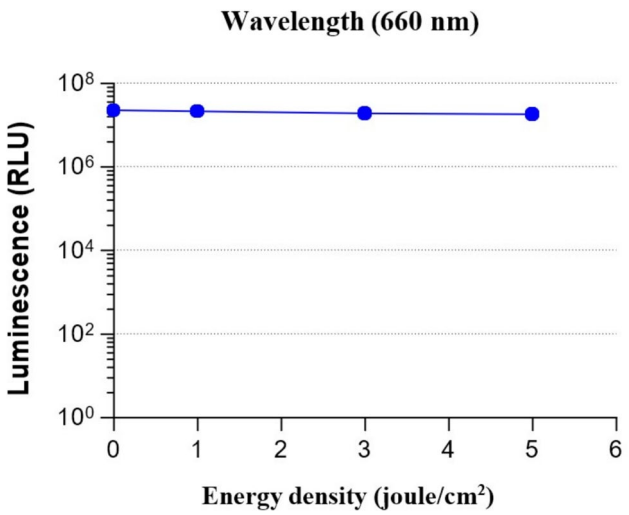

Fig. 13 Control test of the effect of photomodulation on ATP levels (660 nm; 1, 3, 5 J/cm^2). ATP levels in H-6053 human alveolar epithelial cells measured at 72 h using the CellTiter-Glo luminescent assay are shown. Data are normalized to the concurrent dark control and presented as % of control

boundary between the red and near-infrared spectra, led to a balanced increase in all surfactant proteins. Further clinical studies involving experimental animal models and human subjects are necessary to fully elucidate the therapeutic potential of infrared photobiomodulation therapy. Respiratory Distress Syndrome (RDS) remains a serious condition with significant morbidity and mortality rates in premature infants, despite significant advances in its treatment. In this study, we developed a Photobiomodulation (PMB) device that is expected to contribute to increasing surfactant production in the lungs during the early stages of premature birth, thereby preventing complications and problems caused by RDS. It is hoped that this will shorten or prevent the need for intensive care during the neonatal period.

Acknowledgements I would like to thank the Scientific and Technological Research Council of Turkey (TÜBİTAK) for supporting our project SBAG 221S431 and the project team at our university. Patent applications for this device have been filed under national patent number 2023/019371 and international patent number PCT/TR2024/051826.

Author contributions All authors contributed equally to the research and the prepared publication.

Funding The authors declared that this study has received no financial support.

Data availability The data that support the findings of this study are available from the corresponding author upon reasonable request.

Declarations

Conflict of interest The authors declare that there are no competing interests.

Ethical approval Since the research was conducted on cells, no ethics committee approval is required.

References

1. Sweet, D. G., Turner, M. A., Stranak, Z., Plavka, R., Clarke, P., Stenson, B. J., Singer, D., Goelz, R., Fabbri, L., Varoli, G., Piccinno, A., Santoro, D., & Speer, C. P. (2017). A first-in-human clinical study of a new SP-B and SP-C enriched synthetic surfactant (CHF5633) in preterm babies with respiratory distress syndrome. *Archives of Disease in Childhood Fetal and Neonatal Edition, 102*(6), F497–F503. https://doi.org/10.1136/archdischild-2017-312722
2. Özkan, H., Erdeve, Ö., Kanmaz Kutman, H.G. (2018). *Respiratory distress syndrome and surfactant treatment guide*. Turkish Neonatology Society. ISBN: 978-605-68344-0-0. https://doi.org/10.5152/TurkPediatriArs.2018.01806
3. Dilmen, U., Özdemir, R., & Tatar Aksoy, H. (2014). Early regular versus late selective poractant treatment in preterm infants born between 25 and 30 gestational weeks: A prospective randomized multicenter study. *Journal of Maternal-Fetal & Neonatal Medicine, 27*(4), 411–415. https://doi.org/10.3109/14767058.2013.818120
4. Wiingreen, R., Greisen, G., & Ebbesen, F. (2017). Surfactant need by gestation for very preterm babies initiated on early nasal CPAP: A Danish observational multicentre study of 6,628 infants born 2000–2013. *Neonatology, 111*(4), 331–336. https://doi.org/10.1159/000451021
5. Hamblin, M. R. (2016). Shining light on the head: Photobiomodulation for brain disorders. *BBA Clinical, 6*, 113–124. https://doi.org/10.1016/j.bbacli.2016.09.002
6. Lyons, S. K., Patrick, P. S., & Brindle, K. M. (2013). Imaging mouse cancer models in vivo using reporter transgenes. *Cold Spring Harbor Protocols, 2013*(2013), 685–699. https://doi.org/10.1101/pdb.top069864
7. De Cunha, M. G., Vitoretti, L. B., de Brito, A. A., et al. (2018). Low-level laser therapy reduces lung inflammation in an experimental model of chronic obstructive pulmonary disease involving P2X7 receptor. *Oxidative Medicine Cellular Longevity, 2018*, 6798238. https://doi.org/10.1155/2018/6798238
8. Miranda da Silva, C., Peres Leal, M., Brochetti, R. A., et al. (2015). Low level laser therapy reduces the development of lung inflammation induced by formaldehyde exposure. *PLoS ONE, 10*, e0142816. https://doi.org/10.1371/journal.pone.0142816
9. Cury, V., de Lima, T. M., Prado, C. M., Pinheiro, N., Ariga, S. K., Barbeiro, D. F., Moretti, A. I., & Souza, H. P. (2016). Low level laser therapy reduces acute lung inflammation without impairing lung function. *Journal of Biophotonics, 9*, 1199–1207. https://doi.org/10.1002/jbio.201500113
10. Oliveira, M. C., Jr., Greifo, F. R., Rigonato-Oliveira, N. C., et al. (2014). Low level laser therapy reduces acute lung inflammation in a model of pulmonary and extrapulmonary LPS-induced ARDS. *Journal of Photochemistry and Photobiology B: Biology, 134*, 57–63. https://doi.org/10.1016/j.jphotobiol.2014.03.021
11. Griese, M. (1999). Pulmonary surfactant in health and human lung diseases: State of the art. *European Respiratory Journal, 13*(6), 1455–1476. https://doi.org/10.1183/09031936.99.13614779
12. Aguida, B., Pooam, M., Ahmad, M., & Jourdan, N. (2021). Infrared light therapy relieves TLR-4 dependent hyper-inflammation of the type induced by COVID-19. *Communicative & Integrative Biology, 14*(1), 200–211. https://doi.org/10.1080/19420889.2021.1965718

13. Aguida, B., Chabi, M. M., Baouz, S., Mould, R., Bell, J. D., Pooam, M., et al. (2023). Near-infrared light exposure triggers ROS to downregulate inflammatory cytokines induced by SARS-CoV-2 spike protein in human cell culture. *Antioxidants, 12*(10), 1824. https://doi.org/10.3390/antiox12101824
14. Pelletier-Aouizerate, M., & Zivic, Y. (2021). Early cases of acute infectious respiratory syndrome treated with photobiomodulation, diagnosis and intervention: Two case reports. *Clinical Case Reports, 9*, 2429–2437. https://doi.org/10.1002/ccr3.4058
15. Pereira, P. C., de Lima, C. J., Fernandes, A. B., Zangaro, R. A., & Villaverde, A. B. (2023). Cardiopulmonary and hematological effects of infrared LED photobiomodulation in the treatment of SARS-COV2. *Journal of Photochemistry and Photobiology B, Biology, 238*, 112619. https://doi.org/10.1016/j.jphotobiol.2022.112619
16. Jacques, S. L. (2013). Optical properties of biological tissues: A review. *Physics in Medicine and Biology, 58*(11), R37. https://doi.org/10.1088/0031-9155/58/11/r37
17. Karu, T. I., Pyatibrat, L. V., Kolyakov, S. F., & Afanasyeva, N. I. (2005). Absorption measurements of a cell monolayer relevant to phototherapy: Reduction of cytochrome c oxidase under near IR radiation. *Journal of Photochemistry and Photobiology, B: Biology, 81*(2), 98–106. https://doi.org/10.1016/j.jphotobiol.2005.07.002
18. Huang, Y. Y., Chen, A. C. H., Carroll, J. D., & Hamblin, M. R. (2009). Biphasic dose response in low level light therapy. *Dose-Response*. https://doi.org/10.2203/dose-response.09-027.hamblin
19. Hale, G. M., & Querry, M. R. (1973). Optical constants of water in the 200-nm to 200-μ m wavelength region. *Applied Optics, 12*(3), 555–563. https://doi.org/10.1364/ao.12.000555
20. Feng, Z., Tang, T., Wu, T., Yu, X., Zhang, Y., Wang, M., & Qian, J. (2021). Perfecting and extending the near-infrared imaging window. *Light: Science & Applications, 10*(1), Article 197. https://doi.org/10.1038/s41377-021-00628-0

Springer Nature or its licensor (e.g. a society or other partner) holds exclusive rights to this article under a publishing agreement with the author(s) or other rightsholder(s); author self-archiving of the accepted manuscript version of this article is solely governed by the terms of such publishing agreement and applicable law.